Materials and Structures (2009) 42:541–557
DOI 10.1617/s11527-008-9401-y

ORIGINAL ARTICLE

Cement-based piezoelectret

Chiung-Yi Huang · Shoukai Wang · D. D. L. Chung

Received: 7 December 2007 / Accepted: 30 June 2008 / Published online: 5 July 2008

Abstract A cement-based piezoelectret is reported for the first time. Both poling during setting and sodium silicate liquid admixture strengthened the piezoelectret effect. The electret voltage increased upon compressive strain, with partial reversibility; the voltage change was up to 450 V per unit strain (i.e., piezoelectret coupling coefficient up to 4.2×10^{-15} m/V). The effect was relatively strong for a Na^+ concentration of 0.5 M in the water, in combination with a poling electric field of 225 V/m. The effect increased with increasing magnitude of the constant compressive stress. The direct piezoelectric effect was observed as a minor effect, with the voltage decreasing upon compressive strain; the voltage change was up to 6.7 V per unit strain (i.e., piezoelectric coupling coefficient down to -2.3×10^{-16} m/V). An Na^+ concentration of 0.5 M gave superior performance than 1.0 M. For 0.5 M, the compressive modulus and piezoelectret coupling coefficient were higher. The poling reduced the compressive modulus and caused pore formation in the vicinity of the electrodes, but it enhanced the piezoelectret effect.

Keywords Cement · Piezoelectret · Piezoelectric · Poling · Sodium silicate

1 Introduction

The piezoelectret effect [1] (also known as the piezoelectric electret effect [2]) refers to the effect of stress or strain on the voltage across a material, such that the effect is due to the effect of stress or strain on the electret associated with the material. This effect is to be distinguished from the well-known direct piezoelectric effect, which is due to the effect of stress or strain on the electric polarization in the material in the absence of electret formation. However, both the piezoelectret effect and the direct piezoelectric effect are reversible and convert mechanical energy to electrical energy and allow the sensing of stress or strain. This paper provides the first report of a cement-based piezoelectret.

The piezoelectret effect is useful for acoustic emission signal detection [1] and accelerometers [3]. Electrets in the form of polymer films are commercially used in microphones. This application is based on the notion that the electret voltage is affected by the acoustic vibrations. This notion basically involves the concept of the piezoelectret effect. Other applications of electrets (to be distinguished from piezoelectrets) include dust anchoring [4], blood platelet adhesion [5], memories [6], dosimetry of γ-radiation [7] and others [8].

The electret effect has been observed in polymers, particularly polyvinylydene fluoride [9–16], which is attractive for its polar bond and the consequent electric polarizability. It has also been observed in

---

C.-Y. Huang · S. Wang · D. D. L. Chung (✉)
Composite Materials Research Laboratory, University at Buffalo, State University of New York, Buffalo, NY 14260-4400, USA
e-mail: ddlchung@buffalo.edu

ceramics, particularly $Pb(Ti,Zr)O_3$ [17], $CaTiO_3$ [18], $MgO–CaO–SiO_2–Al_2O_3$ [19] and hydroxyapatite [20]. In addition, it has been observed in cement in the absence of ionic admixtures and in the absence of poling [21]. In particular, Panchapakesan [21] observed an inherent voltage in cement after curing in the absence of poling. This inherent voltage and the response of the voltage to a current pulse are indications of the electret effect. The inherent voltage is attributed to slightly inhomogeneous distribution of the ions in the cement paste.

The electret voltage in cement paste has been shown by Huang and Chung [22] to be controlled and increased by electric poling during setting and/or by the use of sodium silicate liquid as an admixture. Therefore, this paper will include investigation of the effects of poling and sodium silicate on the piezoelectret effect.

The piezoelectret effect and the direct piezoelectric effects are different not only in the scientific origin, but also in the performance characteristics. The former involves the voltage in the stress direction increasing upon compression (due to effect of strain on the electret behavior), whereas the latter involves the voltage decreasing upon compression (due to the decrease in the polarization).

The electret behavior originates from an inherent voltage, which exists in the absence of a stress and is due to inherent polarization. The inherent polarization is associated with an inherent separation of the positive and negative charge centers. This separation is due to the difference in the spatial distribution of the positive and negative charges. The special aspect of the electret effect is that the charges associated with the polarization relax and form a core, which then induces surface charge of opposite sign (Fig. 1). It is the surface charge that is responsible for the electret effect. Because the surface charge is opposite in sign from that associated with the inherent polarization, the voltage, as measured by using electrical contacts that are on the surface, changes in opposite directions upon compression for the piezoelectret effect (Fig. 1) and the direct piezoelectric effect (Fig. 2).

The piezoelectret effect in cement-based materials is expected to be valuable for allowing a cement-based structure to sense its stress or strain. Alternate mechanisms of such sensing include the direct piezoelectric effect and the piezoresistive effect. The piezoresistive effect refers to the change in electrical resistivity with strain and has been extensively studied in carbon fiber reinforced cement

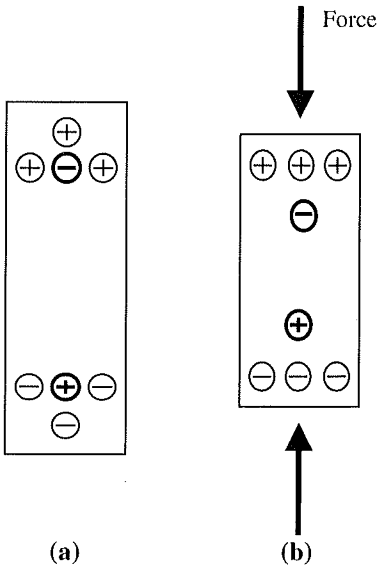

Fig. 1 Possible mechanism of the piezoelectret effect. The bold ions are due to polarization and the others ions are induced by these ions. (**a**) Under no stress. (**b**) Under compression. The strain due to the stress is exaggerated for the sake of illustration

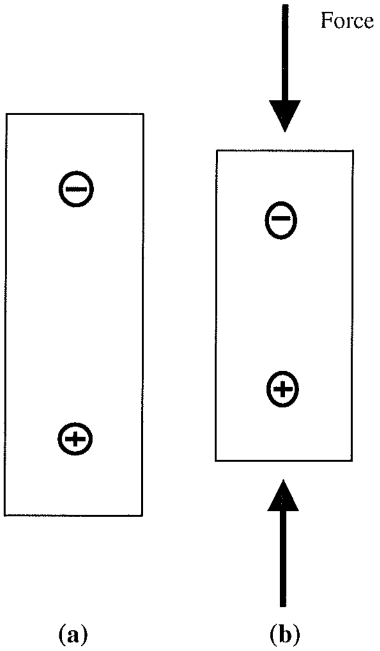

Fig. 2 Mechanism of the piezoelectric effect. (**a**) Under no stress. (**b**) Under compression The strain due to the stress is exaggerated for the sake of illustration

[23–30]. The direct piezoelectric effect has been investigated to a smaller extent in cement-based materials [31–38]. Prior work on the direct piezoelectric effect in cement-based materials emphasizes the use of piezoelectric particle admixtures, such as PZT [34–38]. In addition, it has been observed in cement-based materials without admixture [32, 33].

The charging of a polymer electret may be achieved by the use of corona voltage application [39], electron beam bombardment [39, 40] and triboelectrification [41]. In contrast, the inherent voltage in a cement-based material is due to the non-uniform spatial distributions of the positive and negative ions. This non-uniformity is not a consequence of any special mixing procedure, as the conventional mixing procedure tends to give rise to small degrees of non-uniformity.

Cement is a silicate material, primarily calcium silicate ($3CaO \cdot SiO_2$ and $2CaO \cdot SiO_2$). Ions in cement are responsible for the piezoelectret effect. To increase the ion content, salt such as sodium chloride may be dissolved in the water that is used in a cement mix. However, salt addition is undesirable, due to its negative effect on the durability of cement-based materials, particularly those that contain steel reinforcing bars. Therefore, following Huang and Chung [22], this work used sodium silicate (also known as water glass) as a liquid admixture to enhance the ion content in cement. Sodium silicate has long been used as an admixture in cement for underground construction [42], grout [43–46], waste solidification [46], acid-resistant cement [47], crack diminution admixture [48] and cement sealer [49].

The objectives of this paper are (i) to observe for the first time the piezoelectret effect in cement-based materials and (ii) to investigate the effects of poling and sodium silicate admixture on the piezoelectret effect and on the mechanical behavior.

2 Research approach

2.1 Introduction

This work is an experimental investigation that is directed at observing the piezoelectret effect in cement-based materials for the first time and evaluating this effect. These materials are cement pastes with and without an admixture that provides additional ions to the cement. This admixture is sodium silicate. Furthermore, the effect of poling during setting on the piezoelectret effect is investigated.

Electric poling refers to an electrical process in which an external DC electric field is applied to produce polarization in a material. This process is well-known in case of ferroelectric materials, in which ferroelectric domains are aligned to produce a useful electroactive material that exhibits a net macroscopic polarization.

The experimental approach involves the following aspects.

(i) Cement paste specimens with different proportions of sodium silicate are prepared by mixing and subsequent setting (24 h) and curing (27 days), with the setting step performed optionally in the presence of an applied electric field of 225 V/m (36 V divided the 160-mm length of the specimen) for the purpose of poling. The electric field is applied through electrical contacts in the form of silver coated carbon fiber mat that are located at the end surfaces of the specimen. These end surfaces are perpendicular to the direction of the electric field, which is along the length of the specimen. Each electrical contact covers most of the area of an end surface, so the electric field is essentially uniform throughout the cross section of the specimen. Both setting and curing are performed in a moisture chamber.

(ii) After the setting and during the curing, in the absence of an applied electric field, the voltage across the specimen is monitored as a function of time. This allows study of the process of natural depoling during curing. The voltage is in the same polarity as the poling voltage, indicating that it is not due to polarization, but is due to the electret effect. Thus, the decrease of the voltage with time is an indication of the gradual reduction of the electret effect after the removal of the applied electric field.

(iii) Due to the electrolysis that accompanies the poling process and the consequent generation of gases at the electrodes, the end regions of each specimen in the vicinity of the electrodes are porous and are removed by cutting. The shortened specimen is the form that is evaluated in terms of the piezoelectret effect.

(iv) The piezoelectret effect is evaluated by applying electrical contacts in the form of silver paint (together with a copper foil, such that the copper foil is attached to the specimen using the silver paint) at the two end surfaces and then subjecting the specimen to compression in the direction perpendicular to the end surfaces. The voltage across the two copper foils (at the two end surfaces) and the strain (indicated by a strain gage attached to the center of a side surface of the specimen) in the stress direction are monitored continuously during repeated cycles of loading, a period of constant stress, and subsequent unloading at various stress amplitudes. The cycling allows study of the extent of reversibility of the voltage change and of the strain.

2.2 Experimental methods

2.2.1 Materials

All cement-based materials studied were cement pastes. In other words, no aggregate (fine or coarse) was used. The cement used was Portland cement (Type I, Lafarge, Southfield, MI). Sodium silicate (Na_2SiO_3, liquid, Grade 50, Occidental Chemical Corporation, Dallas, TX) was optionally used as an admixture for providing Na^+ ions. The water–cement ratio was 0.35. In case that sodium silicate is used, a high-range water-reducing agent (Glenium 3000 NS, Degussa Admixture, Cleveland, OH) was used in the amount of 1.0% by mass of cement. A rotary mixer with a flat beater was used for mixing. In the absence of sodium silicate, no water reducing agent was used.

Cement paste specimens with different proportions of sodium silicate were prepared by mixing and subsequent setting (24 h) and then curing (27 days), with the setting step performed optionally in the presence of an applied electric field of either 31 or 225 V/m for the purpose of poling. Demolding occurred immediately after the 24-h setting. After pouring into molds, an external vibrator was used to facilitate compaction and decrease the amount of air bubbles. Immediately after the pouring of the cement mix into the mold, a constant voltage (36 V, unless stated otherwise, corresponding to an electric field of 225 V/m) was optionally applied across the 160-mm length of the specimen during the 24-h setting for the purpose of poling (Fig. 3). The DC power supply used was TO36-10M Regatran Semiconductor Power Supply, The Electronic Measurements Co., Eatontown, NJ. After the 24-h period of setting and optional simultaneous poling, the specimen was demolded and placed in a moisture chamber for 27 days of curing, while the voltage between the two electrical contacts was measured intermittently using a multimeter (30XR, Meterman Test Tools, Everett, WA). Both setting and curing were performed in a moisture chamber at a relative humidity of nearly 100%.

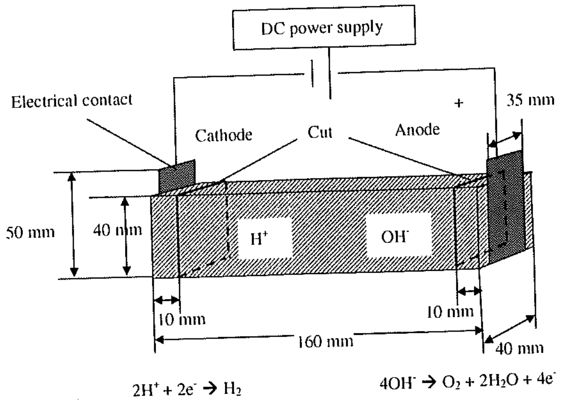

Fig. 3 Specimen configuration for poling

The poling electric field was applied through electrical contacts that were located at the end surfaces of the specimen, i.e., between a specimen end and the proximate polyethylene mold surface. Polyethylene was chosen due to its electrical insulation ability. The mold cavity was of size 160 mm × 40 mm × 40 mm. The end surfaces were perpendicular to the direction of the electric field, which was along the length of the specimen. Each electrical contact covered most of the area of an end surface, so the electric field was essentially uniform throughout the cross section of the specimen.

The electrical contacts were in the form of carbon fiber mat that had been coated with silver paint, as fabricated using the following procedure. Carbon was chosen due to its electrical conductivity and chemical inertness. (The use of copper wire in place of carbon led to undesirable reactions that resembled corrosion at the copper.) A piece of carbon fiber mat (one grammage, 34 g/m^2) was sandwiched by two pieces of carbon fiber mat (two grammage, 8 g/m^2). These mats are wet-laid nonwoven carbon veil, with fibers of length 6 and 12 mm and diameter 7 μm, and binder in the form of polyvinyl alcohol (Grade 20301A, Optimat Carbon Fiber Veil, Technical Fiber Products Inc, Newburgh, NY). Silver paint was manually applied between mats to from the sandwich. In addition, silver paint was applied on the opposite surfaces of the sandwich. Each electrical contact was of size 50 mm × 35 mm and thickness 0.328 mm before application of silver paint at the outer surfaces and 0.38 ± 0.02 mm after application of silver paint at the outer surfaces. The 50-mm length of each electrical contact was along the direction perpendicular to the base of the mold cavity.

The electrochemical reactions that occurred while the cement was setting generated gases (probably O_2 at the anode and H_2 at the cathode), thus causing the formation of large voids around the electrical contacts. The fact that gas evolution occurred at the electrodes during poling suggests the drift of ions in response to the applied electric field was long range rather than short range.

A possible reaction at the anode is the following, though it has not been ascertained.

$$4OH^- \rightarrow O_2 + 2H_2O + 4e^-. \qquad (1)$$

The OH^- ions are inherently present in cement. Reaction (1) generates oxygen gas. A possible reaction at the cathode is the following.

$$2H^+ + 2e^- \rightarrow H_2. \qquad (2)$$

The H^+ ions are present in cement. Reaction (2) generates hydrogen gas.

The gas generation reactions (1) and (2) above do not involve carbon, the electrical contact material. In other words, carbon, which merely serves as an electrical conductor, is not responsible for the gas generation.

Due to the gas evolution at the electrodes, regions at and near the two ends of a specimen were highly porous. Therefore, the end regions were removed by cutting using a wet tile saw prior to testing. After cutting, the specimen length was 140 mm, while the other two dimensions remained the same.

The commercial sodium silicate product was 100% liquid. The solid content was 44.45 wt%, i.e., the proportion of the solid component after heating the product to 1,000°F (540°C). This water amount was included in the total water amount used in the cement mix, so that the water–cement ratio was maintained at 0.35. The composition of each of three cement mixes used is shown in Table 1.

2.2.2 *Testing*

2.2.2.1 Piezoelectret evaluation Each cement specimen was a column of height 140 mm column and cross-section 40 mm × 40 mm (Fig. 4). Two electrical contacts were used for voltage measurement. They were in the form of silver paint in conjunction with copper foil (50 mm × 50 mm × 0.035 mm) were attached to the two end surfaces that were perpendicular to the axis of the column. For each contact, silver paint was applied between the specimen surface and a copper foil.

Piezoelectret evaluation involved measurement of the voltage between the two ends of a specimen during compression loading and unloading, with the stress applied along the axis of the specimen column. During compression of the specimen, each contact was necessarily compressed in the direction perpendicular to the plane of the contact. The compression

Table 1 Ingredients in each of three cement mixes

Admixture	Water excluding that in the sodium silicate product (% by mass of cement)	Sodium silicate product (% by mass of cement)	Water reducing agent (% by mass of cement)
None	35	0	0
Na^+ ions[a] (0.5 M[b])	33	3.63	0
Na^+ ions[a] (1.0 M[b])	31	7.26	1.0

In each case, the total water amount corresponds to a water/cement ratio of 0.35

[a] From sodium silicate admixture

[b] Concentration of Na^+ ions in the water used in the mix

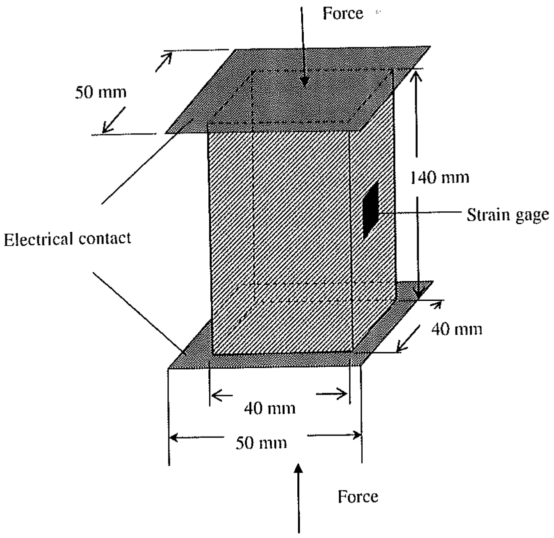

Fig. 4 Specimen configuration for piezoelectret evaluation

was provided by a Sintech 2/D screw-action mechanical testing system. After a selected stress (ranging from 0.70 to 2.23 MPa) had been attained, the stress was maintained constant for a time ranging from 10 to 80 min. In case of a time of 10 min at a constant stress, multiple cycles of loading and unloading were imposed. A strain gage (EA-06-120LZ-120, Measurements Group, Instruments Division, Raleigh, NC) was attached to the specimen surface at the center of the column, as shown in Fig. 4, for monitoring the strain in the stress direction during loading and unloading. A multimeter (Keithley 2002, Cleveland, OH) was used to measure the voltage.

2.2.2.2 Mechanical testing The mechanical behavior was studied by compressive testing in the poling direction. Each specimen was obtained by cutting a specimen of size 160 × 40 × 40 mm, such that the center portion of size 40 × 40 × 40 mm was obtained. A strain gage (Cat. No. EA-06-120LZ-120, Vishay Measurements Group, Raleigh, NC) was attached to the center of a face of the cubic specimen surface, with the face being parallel to the poling direction. Compressive stress was applied repeatedly, such that the stress amplitude progressively increased in the order: 0.84, 1.67, 2.51, 3.34, 4.18 and 5.01 MPa. The maximum stress in each stress cycle was maintained for 5 min. The displacement rate during loading and unloading was 0.5 mm/min. The slope of the stress–strain curve during loading gave the modulus, which describes the elastic behavior. The rate of change of the strain in the period of constant stress described the inelastic behavior.

2.2.2.3 Relative dielectric constant measurement The relative dielectric constant was measured at 1 kHz by using a Precision RLC meter (QuadTech, Inc., Maynard, MA, Model 7600). Specimens without poling were tested. Each specimen was a disc of thickness 2.0 mm and diameter 12.7 mm, sandwiched by two copper discs, each of thickness 3.0 mm and diameter 12.7 mm, at a sandwiching pressure of 1.68 kPa. The amplitude of the voltage between the two copper discs was 1.000 V. Between the specimen and each of the two copper discs was a polytetrafluoroethylene (Teflon) sheet (thickness 0.025 mm) that served as an electrical insulator. The capacitance of this parallel-plate capacitor was measured and the relative dielectric constant was calculated from the capacitance and the specimen dimensions. The capacitance was obtained using two methods, i.e., (i) C_p, which was obtained by assuming an equivalent circuit consisting of a capacitor and a resistor in parallel and (ii) C_s, which was obtained by assuming an equivalent circuit consisting of a capacitor and a resistor in series. These two values of the capacitance were used to calculate the corresponding values of the relative dielectric constant.

3 Results and discussion

3.1 Electret behavior

The voltage was measured across the specimen by using the same electrical contacts as in poling. The poling was carried out only during setting (24 h)—not during the subsequent curing. After poling, the voltage was monitored in the absence of an electric field up to 27 days of curing for the purpose of investigating the stability of the electret formed by the poling.

Immediately after removal of the poling voltage at the end of the 24-h setting period, the specimen was demolded and measurement of the voltage across the specimen was immediately started. The measured voltage was positive for all compositions and all poling conditions, as shown in Table 2. This means

Table 2 Voltage across the specimen, measured during curing with the electric field off

Na^+ concentration (M)	Poling electric field (V/m)	Measured voltage (V)		Voltage at 28 days divided by that at 1 day
		1 day[a]	28 days[b]	
0	0	0.007	0.003	0.429
0	0	−0.001	0.003	−3.22
0	0	−0.001	−0.004	3.82
0	31	0.90	0.04	0.044
0	31	0.89	0.02	0.022
0	225	1.39	−0.16	–
0	225	1.40	−0.40	–
0	225	1.20	−0.10	–
0.5	225	0.74	0.18	0.243
0.5	225	0.90	0.18	0.200
0.5	225	0.90	0.22	0.244
1.0	225	0.67	0.31	0.463
1.0	225	0.86	0.35	0.407
1.0	225	0.86	0.33	0.384

The voltage is in the same polarity as the poling voltage

[a] Immediately after 1 day of setting

[b] After 1 day of setting, followed by 27 days of curing

that the measured voltage had the same polarity as the poling voltage, indicating that the voltage was due to electret formation. However, the electret stability differed among the various compositions and the various poling conditions. In the absence of sodium silicate, poling with a voltage of 5.0 V (electric field of 31 V/m) resulted in an increased electret effect (Table 2). However, an increase in the poling voltage from 5 to 36 V caused the polarization effect to overshadow the electret effect, so that the measured voltage was negative at 28 days of curing (Table 2). For a poling voltage of 36 V (electric field of 225 V/m), an increase of the sodium silicate concentration from 0 to 1.0 M increased the electret stability, as shown by an increased value of the ratio of the electret voltage at 28 days to that at 1 day (Table 2). Thus, both poling and sodium silicate helped the formation of a stable electret.

3.2 Mechanical behavior

Figures 5–9 show the variation of the stress with time and of the strain with time during repeated compressive loading at progressively increasing stress amplitudes for the specimen types listed in Table 2. In addition, they show, for each specimen type, the compressive stress–strain curve during loading and subsequent unloading for various values of the maximum stress. Each specimen type is characterized by its combination of poling electric field and sodium ion concentration. These plots provide information on the elastic behavior (variation of the strain with stress in the period of increasing stress) and the inelastic behavior (variation of the strain with time in the period of constant stress in each cycle). The strain is not totally reversible upon unloading, even for the lowest value of the maximum stress. Furthermore, the strain tends to increase with time in the period of constant stress.

Table 3 compiles the data for the elastic behavior. Poling decreases the modulus, whether sodium ions are present or not, presumably because the nonuniformity in the ion concentration after poling. Increase of the Na^+ concentration from 0 to 0.5 M increases the modulus, whether poling has taken place or not. This is probably because of the sealing ability of the sodium silicate. However, further increase of the Na^+ concentration from 0.5 to 1.0 M decreases the modulus.

Table 4 compiles the data for the inelastic behavior, which is described in terms of the strain rate at a constant stress for each of six values of the constant stress. The strain rate is not much affected by the poling or the sodium ion concentration, except that an Na^+ concentration of 1.0 M greatly increases the strain rate. This high strain rate correlates with a low modulus (Table 3). This means that a high sodium silicate concentration is detrimental to the mechanical properties.

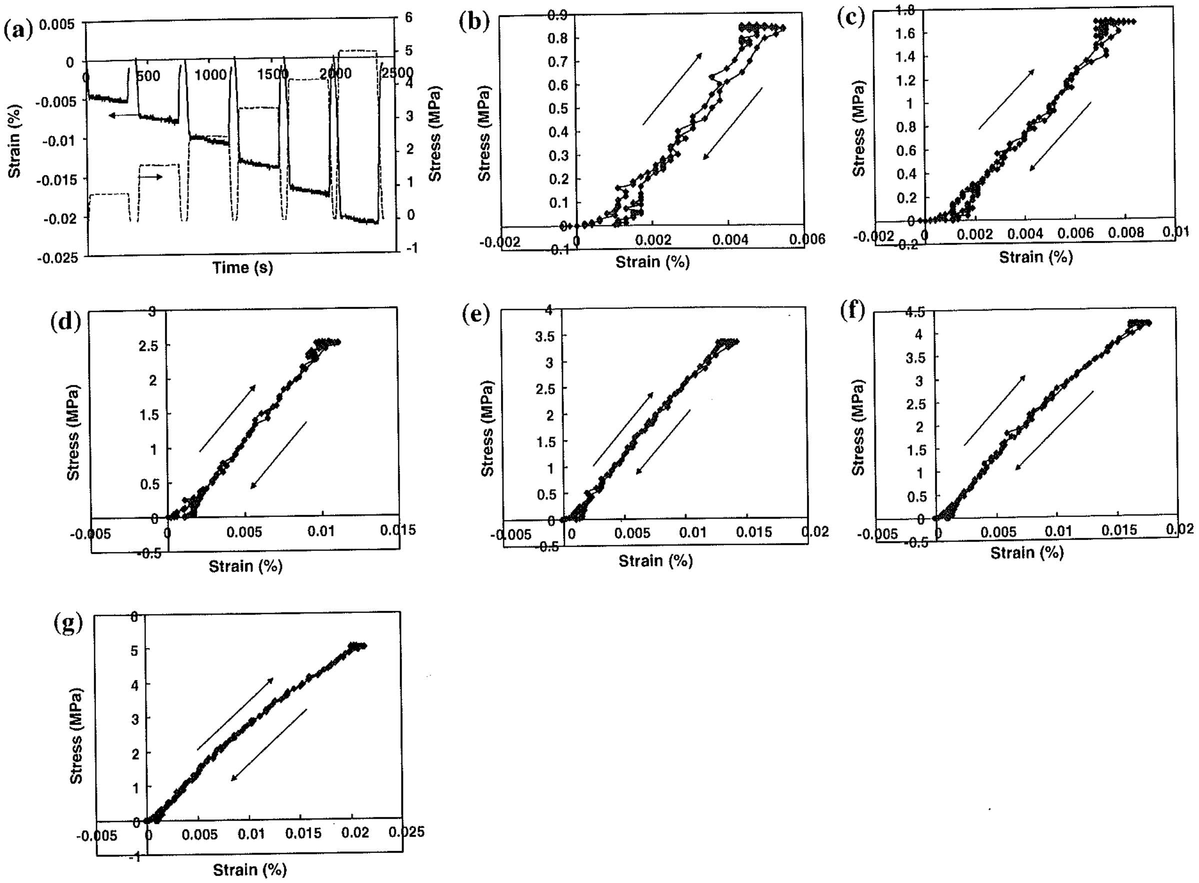

Fig. 5 Mechanical behavior for plain cement (without sodium silicate) in the absence of a poling electric field. (**a**) Strain versus time and stress versus time for progressively increasing values of the maximum stress. Stress–strain curve for a maximum stress of (**b**) 0.84 MPa, (**c**) 1.67 MPa, (**d**) 2.51 MPa, (**e**) 3.34 MPa, (**f**) 4.18 MPa, and (**g**) 5.01 MPa

3.3 Relative dielectric constant

Table 5 shows that the relative dielectric constant, whether based on C_p or C_s, is essentially not affected by the sodium ion content, in spite of the ion concentration increase provided by the sodium silicate. This is attributed to the sealing effect of sodium silicate [49] and the consequent increased restriction of the ion movement. This sealing effect overshadowed the effect of increased ion content, as the sodium silicate proportion increased.

3.4 Piezoelectret behavior

Table 6 describes the piezoelectret effect under compression at a constant stress of 1.81 MPa, which was applied for 80 min, for various combinations of composition and poling electric field. The strain was negative, due to the compression. During the period of constant stress, the measured voltage as well as the compressive strain increased. The increase in compressive strain at a constant stress is due to inelastic deformation. In case of the voltage (measured with the same polarity as the poling voltage) prior to loading being negative, the voltage changed sign (from negative to positive) during the period of constant stress (Fig. 10). In case of the voltage prior to loading being positive, the voltage just increased without changing sign during the period of constant stress.

The strength of the effect is described by the change in measured voltage per unit strain during the period of constant stress. Both the poling voltage and the sodium silicate strengthen the effect (Table 6).

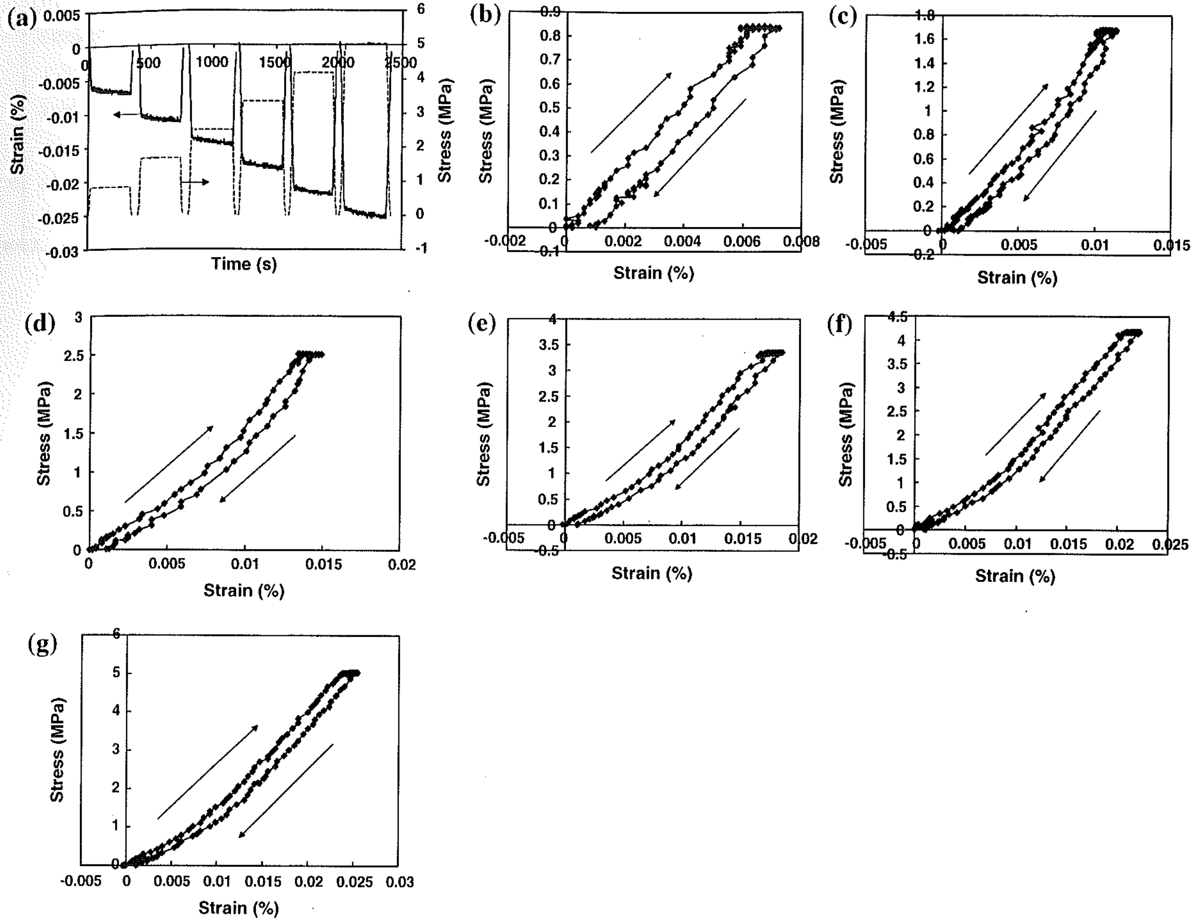

Fig. 6 Mechanical behavior for plain cement (without sodium silicate) after poling at 225 V/m. (**a**) Strain versus time and stress versus time for progressively increasing values of the maximum stress. Stress–strain curve for a maximum stress of (**b**) 0.84 MPa, (**c**) 1.67 MPa, (**d**) 2.51 MPa, (**e**) 3.34 MPa, (**f**) 4.18 MPa, and (**g**) 5.01 MPa

The effect is strongest for an Na^+ concentration of 0.5 M in combination with a poling electric field of 225 V/m, as shown in Fig. 10.

Increase of the Na^+ concentration from 0 to 0.5 M strengthens the effect, but further increase of the Na^+ concentration from 0.5 to 1.0 M diminishes the effect (Table 6). The complex dependence of the strength of the piezoelectret effect on the Na^+ concentration is due to the effects of the Na^+ concentration on the mechanical properties and on the relative dielectric constant. The low strength of the piezoelectret effect at an Na^+ concentration of 1.0 M is partly due to the poor mechanical properties at this concentration (Sect. 3.2) and partly due to the low value of the relative dielectric constant at this concentration (Sect. 3.3).

Table 7 shows that the strength of the effect increased with increasing magnitude of the constant compressive stress. This effect of the stress is mainly due to the increase in the extent voltage change upon increase in the stress, as the strain change varies with the stress only in a limited away.

Upon loading (i.e., during the period of increasing stress rather than constant stress), the voltage decreased, with the voltage change per unit strain up to 6.70 V (Table 8; Fig. 10). Both the voltage decrease and the compressive strain increase during loading were largely reversible upon unloading. The strain effect relates to elastic deformation.

The voltage baseline becomes more and more positive as repeated stress cycling takes place. This baseline increase is because of the superposition of

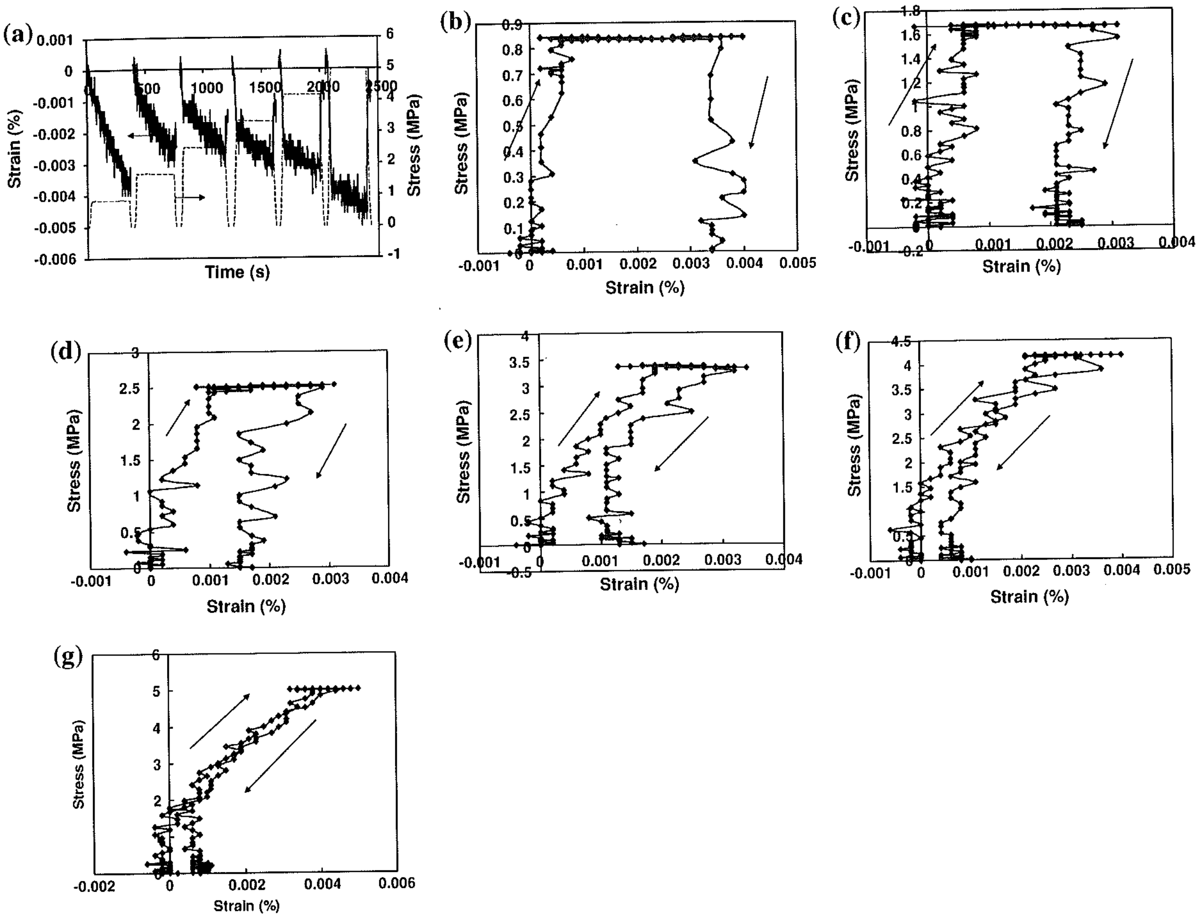

Fig. 7 Mechanical behavior for cement with 0.5 M Na^+ ions in the absence of a poling electric field. (**a**) Strain versus time and stress versus time for progressively increasing values of the maximum stress. Stress–strain curve for a maximum stress of (**b**) 0.84 MPa, (**c**) 1.67 MPa, (**d**) 2.51 MPa, (**e**) 3.34 MPa, (**f**) 4.18 MPa, and (**g**) 5.01 MPa

the effect associated with the voltage increasing with the compressive strain during the period of constant stress to the effect associated with the voltage decreasing with the compressive strain during stress increase (Fig. 11).

The effect of the voltage decreasing with increasing compressive strain during the period of stress increase is the minor effect, as shown by the relatively small magnitude of the voltage change per unit strain (Table 9). In contrast, the effect associated with the voltage increasing with compressive strain in the period of constant stress is the major effect, as shown by a relatively large magnitude of the value of the voltage change per unit strain (Table 7). The major effect is more significant in Fig. 10 than Fig. 11 because the time at constant stress was only 10 min in Fig. 11, but was 60 min in Fig. 10. Due to the difference in the time at constant stress, the strain change in this period is much larger in Fig. 10 than Fig. 11. In Fig. 10, due to the long time at a constant stress, the major effect dominates and the minor effect is only slightly present, if at all.

The major effect described above is the piezoelectret effect, whereas the minor effect described above is the direct piezoelectric effect. In the piezoelectret effect, the voltage increases upon compression (Fig. 1); in the direct piezoelectric effect, the voltage decreases upon compression (Fig. 2).

The direct piezoelectric effect has been previously reported in cement mortar without admixture or poling [33]. The piezoelectret effect has not been

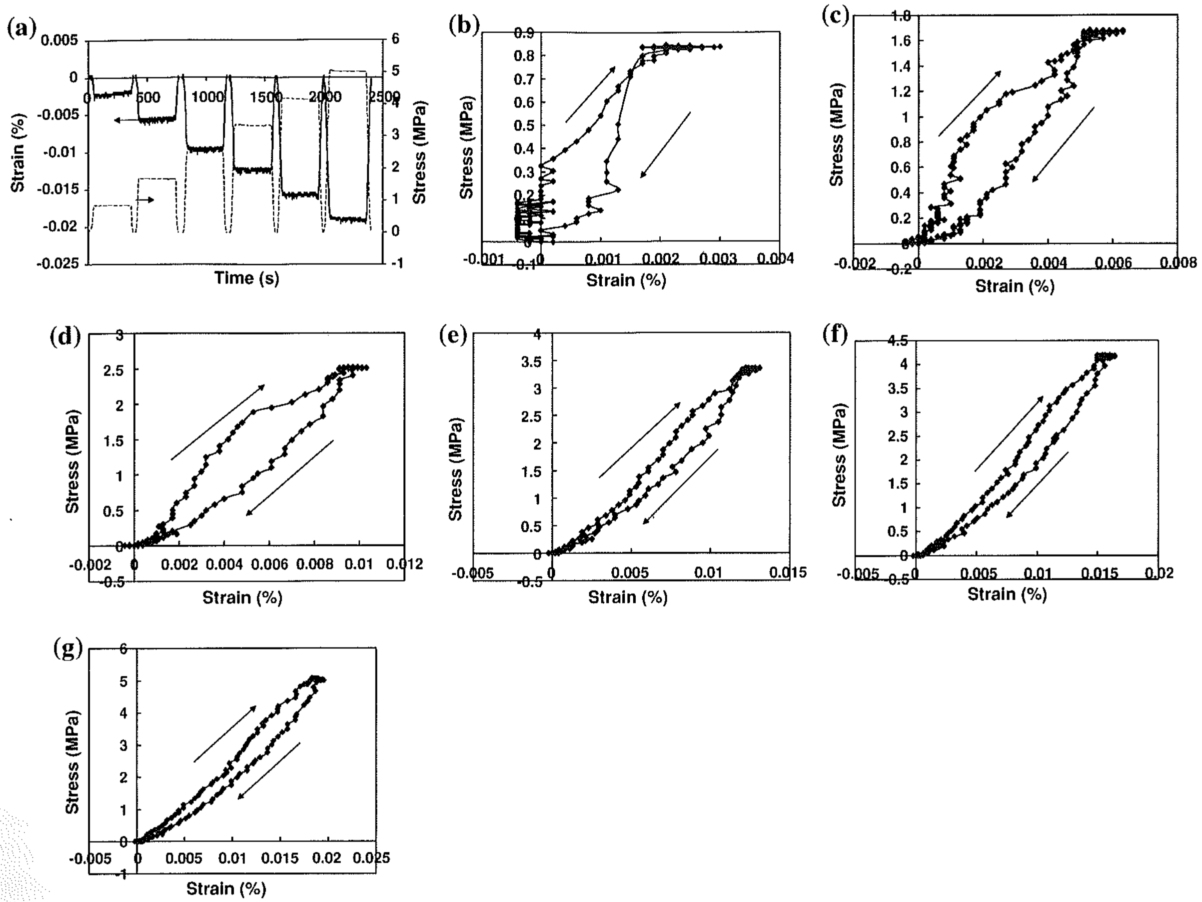

Fig. 8 Mechanical behavior for cement with 0.5 M Na^+ ions after poling at 225 V/m. (**a**) Strain versus time and stress versus time for progressively increasing values of the maximum stress. Stress–strain curve for a maximum stress of (**b**) 0.84 MPa, (**c**) 1.67 MPa, (**d**) 2.51 MPa, (**e**) 3.34 MPa, (**f**) 4.18 MPa, and (**g**) 5.01 MPa

previously reported, but it is suggested by the data in [33]. Figure 5 of [33] resembles Fig. 11 of this work, but it does not show the irreversible deformation that is associated with the piezoelectret effect and is shown in Fig. 11.

The piezoelectret effect is more sluggish than the direct piezoelectric effect, as shown by the longer time the piezoelectret effect takes to occur and the lower degree of reversibility of the piezoelectret effect compared to the direct piezoelectric effect. The sluggishness is probably due to the charge relaxation and induction associated with the piezoelectret effect.

Table 8 shows that, in the period of stress increase, the change in voltage per unit strain is increased only slightly upon poling at a fixed Na^+ concentration of 0.5 M. However, for a fixed poling electric field, the sodium ion concentration strongly affects the change in voltage per unit strain; the change in voltage per unit strain increases significantly when the Na^+ concentration increases from 0 to 0.5 M, and decreases when this concentration is further increased from 0.5 to 1.0 M. Hence, a high value of the change in voltage per unit strain during stress increase (Table 8) correlates with a high value of the change in voltage per unit strain in the period of constant stress (Table 7).

The piezoelectret effect is not completely reversible upon unloading. Table 9 shows that the reversible and irreversible components, as described respectively by the reversible voltage change per unit reversible strain change and the irreversible voltage change per unit

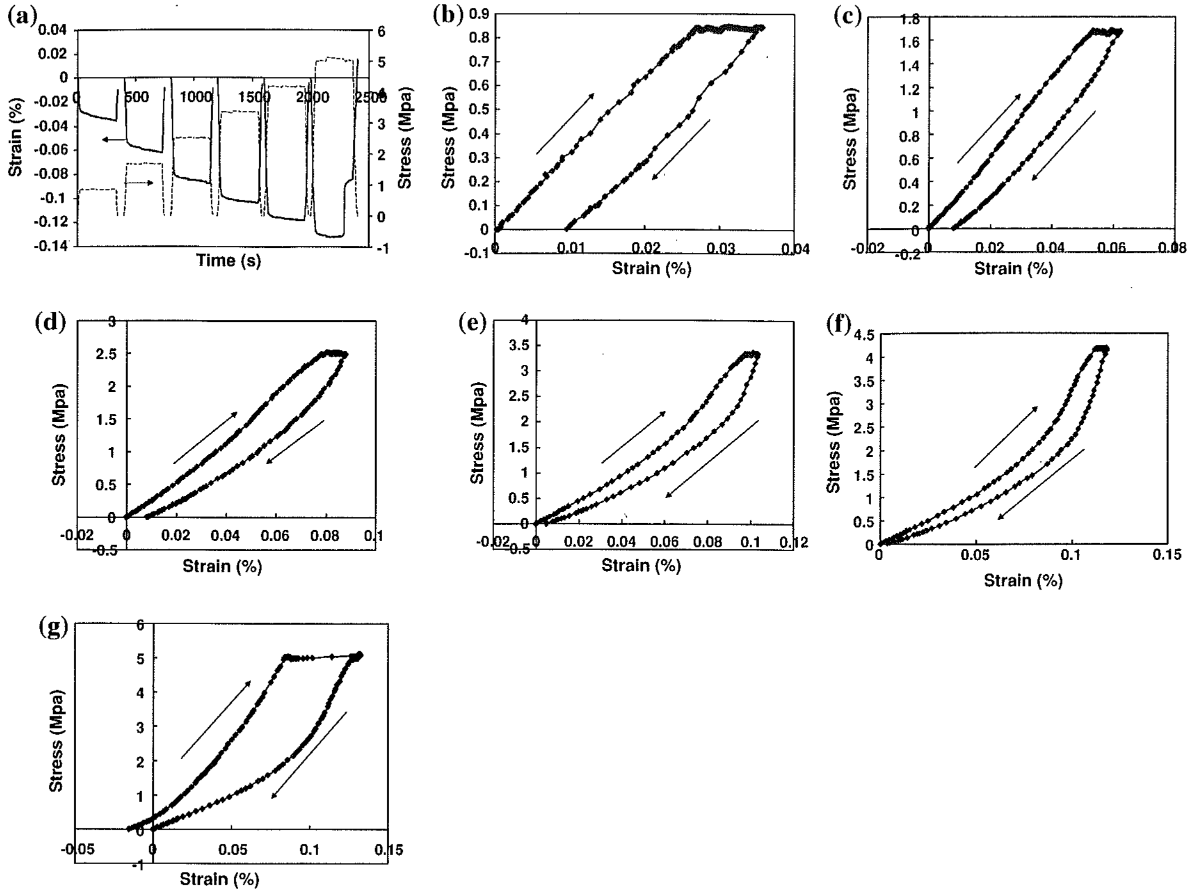

Fig. 9 Mechanical behavior for cement with 1.0 M Na^+ ions after poling at 225 V/m. (**a**) Strain versus time and stress versus time for progressively increasing values of the maximum stress. Stress–strain curve for a maximum stress of (**b**) 0.84 MPa, (**c**) 1.67 MPa, (**d**) 2.51 MPa, (**e**) 3.34 MPa, (**f**) 4.18 MPa, and (**g**) 5.01 MPa

Table 3 Compressive modulus (GPa) for various values of the maximum stress (ranging from 0.84 to 5.01 MPa) for different types of specimen

Na^+ concentration (M)	Poling electric field (V/m)	0.84 MPa	1.67 MPa	2.51 MPa	3.34 MPa	4.18 MPa	5.01 MPa
0	0	18 ± 3	24 ± 1	25 ± 3	25 ± 1	24 ± 2	23 ± 2
0.5	0	50 ± 20	56 ± 19	54 ± 20	54 ± 16	57 ± 14	46 ± 25
0.5	0	53 ± 30	52 ± 27	63 ± 33	57 ± 36	50 ± 31	52 ± 15
0	225	13 ± 1	13 ± 2	13 ± 1	14 ± 1	14 ± 3	14 ± 2
0	225	16 ± 2	16 ± 3	17 ± 1	17 ± 1	17 ± 2	17 ± 3
0.5	225	20 ± 4	25 ± 5	30 ± 3	29 ± 4	27 ± 3	24 ± 4
0.5	225	22 ± 6	29 ± 3	26 ± 5	28 ± 4	28 ± 4	28 ± 3
1.0	225	4.0 ± 0.3	4.0 ± 0.3	4.0 ± 0.3	4.0 ± 0.4	4.0 ± 0.2	4.0 ± 0.4
1.0	225	3.0 ± 0.1	3.0 ± 0.1	3.0 ± 0.2	3.0 ± 0.4	4.0 ± 0.3	4.0 ± 0.4

The modulus is obtained from the initial slope of the stress–strain curve from zero stress to the maximum stress

Table 4 The strain rate (10^{-8} s^{-1}) in the period of constant compressive stress for different combinations of stress and specimen type

Na^+ concentration (M)	Poling electric field (V/m)	0.84 MPa	1.67 MPa	2.51 MPa	3.34 MPa	4.18 MPa	5.01 MPa
0	0	−3.5 ± 0.8	−2.2 ± 0.5	−2.6 ± 0.6	−2.3 ± 0.4	−3.2 ± 0.7	−3.7 ± 0.9
0.5	0	−5.4 ± 1.2	−2.5 ± 0.5	−4.0 ± 0.3	−1.3 ± 0.6	−1.3 ± 0.4	−1.4 ± 0.6
0.5	0	−4.0 ± 0.5	−5.6 ± 0.6	−3.6 ± 0.4	−3.6 ± 0.6	−3.0 ± 0.7	−3.9 ± 0.4
0	225	−2.5 ± 0.3	−3.2 ± 0.4	−3.4 ± 0.6	−3.6 ± 0.4	−4.3 ± 0.5	−4.0 ± 0.8
0	225	−1.6 ± 0.6	−4.1 ± 0.8	−3.0 ± 0.5	−2.3 ± 0.7	−3.5 ± 0.9	−2.9 ± 0.5
0.5	225	−1.9 ± 0.4	−6.2 ± 0.7	−6.3 ± 0.4	−5.2 ± 0.8	−4.2 ± 0.3	−11.6 ± 0.8
0.5	225	−1.3 ± 0.6	−0.6 ± 0.7	−0.7 ± 0.6	−1.3 ± 0.8	−3.2 ± 0.8	−4.2 ± 0.9
1.0	225	−8.2 ± 0.7	−8.0 ± 0.5	−14.9 ± 1.3	−17.6 ± 1.1[a]	−1.4 ± 0.6[a]	−6.1 ± 0.6[a]
1.0	225	−28.2 ± 2.2	−29.1 ± 2.8	−25.8 ± 1.9	−16.9 ± 1.7	−17.4 ± 1.9	−11.4 ± 1.5[a]

[a] The specimen fractured during the mechanical testing at this stress amplitude

Table 5 Relative dielectric constant (κ) in the absence of poling

Na^+ concentration (M)	κ (based on C_p)	κ (based on C_s)
0	20.6 ± 1.0	20.9 ± 1.4
0.5	20.3 ± 1.5	20.5 ± 1.7
1.0	20.1 ± 2.7	20.4 ± 2.8

irreversible strain change during a constant stress of 1.81 MPa, were comparable for an Na^+ concentration of 0.5 M, whether the poling electric field voltage was 0 or 225 V/m. For Na^+ concentrations of 0 or 1.0 M, the irreversible portion dominated. This may be related to the effect of sodium silicate concentration on the mechanical properties of the cement paste. In contrast, the direct piezoelectric effect is quite reversible, as shown in Fig. 11.

The piezoelectret (piezoelectric) coupling coefficient is defined as

$$d = \frac{\varepsilon_0(\kappa - 1)\partial V}{l\partial\sigma},$$

where κ is the relative dielectric constant, d the piezoelectret (piezoelectric) coupling coefficient, l the length of the specimen in the direction of polarization, ∂V the change in voltage, $\partial\sigma$ the change in stress, and ε_0 is the permittivity of free space, which is equal to 8.85×10^{-12} F/m.

In case of 0.5 M Na^+ concentration in combination of a poling electric field of 225 V/m, the piezoelectret coupling coefficient is 4.2×10^{-15} (C/N or m/V), since $l = 0.14$ m, $\partial V = 0.0636$ V (Table 6), $\partial\sigma = 1.81$ MPa and κ (based on C_s) = 20.5, and the piezoelectric coupling coefficient is -2.3×10^{-16} (C/N or m/V), since $l = 0.14$ m, $\partial V = -0.004448$ V (Table 8), $\partial\sigma = 2.32$ MPa and κ (based on C_s) = 20.5.

Table 10 lists the piezoelectret and piezoelectric coupling coefficients for the various combinations of Na^+ concentration and poling electric field. The values of the piezoelectret coupling coefficient are all much higher than those of the piezoelectric coupling coefficient, due to the fact that the piezoelectret effect is the major effect while the piezoelectric effect is the minor effect. In each case, the values based on C_s and C_p are close.

Both piezoelectret and piezoelectric coupling coefficients are increased in magnitude by poling

Table 6 Change in voltage per unit strain under a constant stress of 1.81 MPa, which was applied for 80 min

Na^+ concentration (M)	Poling electric field (V/m)	Change in voltage (V)	Maximum strain (%)	Change in voltage (V) per unit strain under constant stress
0.5	0	0.0257	−0.0218	−164
0	225	0.0040	−0.0440	−37
0.5	225	0.0636	−0.0797	−454
1.0	225	0.0155	−0.0422	−101

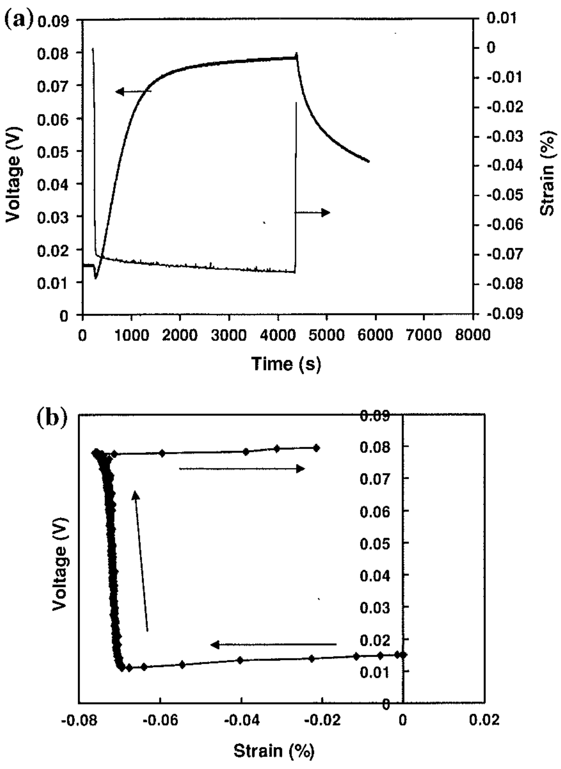

Fig. 10 Piezoelectret behavior for a Na^+ concentration of 0.5 M in combination with a poling electric field of 225 V/m. The behavior was observed during a single cycle of compressive loading at a stress amplitude of 1.81 MPa. The constant stress application time was 70 min. (**a**) Variation of the measured voltage with time and of the strain with time at a constant stress of 1.81 MPa. The increase in voltage is due to the piezoelectret effect and the increase in compressive strain magnitude is due to inelastic deformation. (**b**) Relationship of the measured voltage with strain during one cycle of loading and unloading

and by increase of the Na^+ concentration from 0 to 0.5 M. However, further increase of the Na^+ concentration from 0.5 to 1.0 M decreases the values. These trends reflect similar trends in Tables 6 and 8 for the piezoelectret and piezoelectric effects respectively.

The common piezoelectric materials are quartz, $BaTiO_3$, PZT and $PbNb_2O_6$. The values of their piezoelectric coupling coefficient d_{33} are 2.3×10^{-12}, 1.90×10^{-10}, 2.68×10^{-10} -4.80×10^{-10} and 8×10^{-11} m/V, respectively [50]. No value of the piezoelectret coupling coefficient has been previously reported for any material The values of both piezoelectret and piezoelectric coupling coefficients, as shown in Table 10, are much lower in magnitude than the values mentioned above for typical piezoelectric materials. That the values of the piezoelectric coupling coefficient (Table 10) are low in this work is because of the fact that the piezoelectric effect is a minor effect.

4 Conclusion

The electret effect in cement has been previously established. This paper provides the first observation of the piezoelectret effect in cement-based materials. No aggregate was used. Both poling during the setting of the cement mix and the use of sodium silicate as an admixture helped the formation of a stable electret and strengthened the piezoelectret effect. In this effect, the voltage increased upon compressive strain, with partial reversibility, such that the voltage change was up to 450 V per unit strain, corresponding to a piezoelectret coupling coefficient up to 4.2×10^{-15} m/V (based on C_s). The effect was relatively strong for a Na^+ concentration of 0.5 M in the water used in the cement mix, in combination with a poling voltage of 36 V (225 V/m). The strength of the effect increased with increasing magnitude of the constant compressive stress. The direct piezoelectric effect was also observed, though it was a minor effect, with the voltage decreasing upon compressive strain, such that the voltage change was up to 6.7 V per unit strain, corresponding to a piezoelectric coupling coefficient down to -2.3×10^{-16} m/V (based on C_s).

Table 7 Change in voltage per unit strain under constant stress, which was applied for 80 min

Constant stress (MPa)	Change in voltage (V)	Maximum strain (%)	Change in voltage (V) per unit strain under constant stress
0.70	0.0048	−0.0324	−39
1.25	0.0121	−0.0256	−72
1.81	0.0155	−0.0422	−101

The Na^+ concentration is 1.0 M. The poling electric field is 225 V/m

Table 8 Change in voltage per unit strain during stress increase for the first cycle of compressive loading

Na^+ concentration (M)	Poling electric field (V/m)	Change in stress (MPa)	Change in voltage (mV)	Change in strain (%)	Change in voltage (V) per unit strain
0	225	1.81	−0.186	−0.0104	1.79
0.5	0	1.81	−0.413	−0.0064	6.45
0.5	225	2.32	−4.448	−0.0664	6.70
1.0	225	1.81	−0.999	−0.0173	5.77

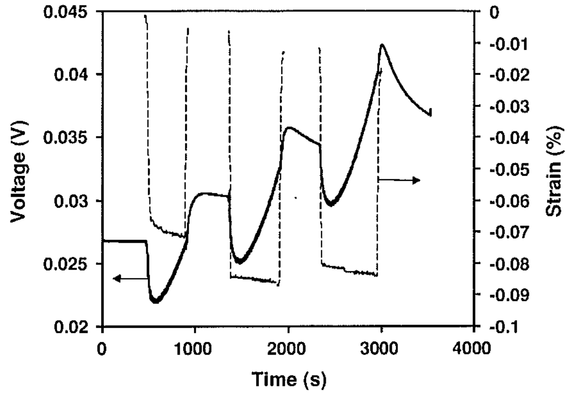

Fig. 11 Piezoelectret behavior for a Na^+ concentration of 0.5 M in combination with a poling electric field of 225 V/m, as observed during three cycles of compressive loading at a stress amplitude of 2.23 MPa. The constant stress application time in each cycle was 10 min. The voltage decreased with increasing compressive strain magnitude during the period of stress increase (piezoelectric effect). The voltage baseline became more and more positive when stress cycling progressed. This baseline increase is due to the voltage increasing with the compressive strain in the period of constant stress

The poling reduced the compressive modulus and caused pore formation in the vicinity of the two electrodes used for electric field application during poling. However, it enhanced the electret effect by increasing the magnitude and stability of the voltage. In addition, it enhanced the piezoelectret effect by increasing the extent of voltage change in response to strain.

An Na^+ concentration of 0.5 M gives superior performance than that of 1.0 M. For 0.5 M, the compressive modulus and piezoelectret coupling coefficient are higher.

Although sodium silicate provided Na^+ ions, the relative dielectric constant (without poling) was essentially not affected by the sodium silicate. This is due to the known sealing effect of sodium silicate.

Table 9 Reversible voltage change per unit reversible strain change and irreversible voltage change per unit irreversible strain change during a constant stress of 1.81 MPa, which was applied for 80 min, for various combinations of sodium ion concentration and poling electric field

Na^+ concentration (M)	Poling electric field (V/m)	Reversible voltage change/ reversible strain change (V)	Irreversible voltage change/ irreversible strain change (V)
0	225	−5	−17
0.5	0	−119	−119
0.5	225	−80	−78
1.0	225	−18	−71

Table 10 Piezoelectret and piezoelectric coupling coefficients

Na^+ ion concentration (M)	Poling electric field (V/m)	Piezoelectret coupling coefficient (10^{-16} m/V)		Piezoelectric coupling coefficient (10^{-17} m/V)	
		C_p	C_s	C_p	C_s
0.5	0	17	17	−2.7	−2.7
0	225	2.6	2.7	−1.2	−1.2
0.5	225	41	42	−22	−23
1.0	225	9.9	10	−6.4	−6.5

Acknowledgment Partial support by the Mark Diamond Research Fund, University at Buffalo, State University of New York, is acknowledged.

References

1. Wenger MP, Blanas P, Shuford RJ, Das-Gupta DK (1996) Acoustic emission signal detection by ceramic/polymer composite piezoelecrets embedded in glass-epoxy laminates. Polym Eng Sci 36(24):2945–2954. doi:10.1002/pen.10696
2. Schwödiauer R, Neugschwandtner GS, Schrattbauer K, Lindner M, Vieytes M, Bauer-Gogonea S et al (2000)

Preparation and characterization of novel piezoelectric and pyroelectric polymer electrets. IEEE Trans Dielectr Electr Insul 7(4):578–586. doi:10.1109/94.868080

3. Meschia SC, Schmidt VH, Taubner S (1996) An electret accelerometer for use in active vibration control systems. In: ISAF'96 proceedings of the IEEE international symposium on applications of ferroelectrics, 10th, East Brunswick, NJ, August 18–21, 1996, vol 1, pp 117–119
4. Gaynor PT, Hughes JF (1998) Dust anchoring characteristics of electret fibers with respect to Der p 1 allergen carrying particles. Med Biol Eng Comput 36(5):615–620. doi:10.1007/BF02524433
5. Shumakov VI, Chepurov AK, Kazlove VK, Kazakova TI (1975) Adhesion of blood platelets to electret polymers. Polim Med 5(3):247–252
6. Scott JF, Zubko P (2005) Electret effects in ferroeletric thin films. In: Proceedings—international symposium on electrets (ISE 12), 12th, Salvador, Brazil, September 11–14, 2005, pp 113–115
7. Magerramov AM, Kerimov MK, Hamidov EM (2004) Electret polymer materials for dosimetry of γ-irradiation. In: NATO Science Series, IV: earth and environmental sciences, p 41. Radiation Safety Problems in the Caspian Region, pp 205–209
8. Bauer S, Bauer-Gogonea S, Dansachumller M, Graz I, Leonhartsberger H, Salhofer H et al (2003) Modern electrets. In: Proceedings—IEEE ultrasonics symposium, vol 1, pp 370–376
9. Sahu DK, Khare PK, Shrivastava RK (2004) Dielectric loss factor in electrically polarized polyvinylidene fluoride film electrets by TSDC. Indian J Phys 78(11):1205–1209
10. Khare PK, Sahu DK, Verma A, Srivatava RK (2004) Depolarization studies of polyvinylidene fluoride foil electrets using thermally stimulated discharge. Indian J Pure Appl Phys 42(9):693–696
11. Fedosov SN, Sergeeva AV, Giacometti JA, Ribeiro PA (1999) Corona poling of a ferroelectric polymer (PVDF). In: Proceedings of SPIE—the international society for optical engineering, p 4017. Polym Liq Crystals 53–58
12. Holstein P, Leister N, Weber U, Geschke D, Binder H, Monti GA et al (1999) A combined study of polarization in PVDF. In: Proceedings—international symposium on electrets, 10th, Delphi, Greece, September 22–24, 1999, pp 509–512
13. Eisenmenger W, Schmidt H, Dehlen B (1999) Space charge and dipoles in polyvinylidene fluoride. Braz J Phys 29(2):295–305. doi:10.1590/S0103-97331999000200011
14. Frensch H, Wendorff JH (1985) Correlations between the structure and the electret behavior of PVDF/PMMA alloys. In: Proceedings—international symposium on electrets, 5th, pp 132–137
15. Sessler GM, Gerhard-Multhaupt R, Von Seggern H (1985) Charge and polarization profiles in polymer electrets. In: Proceedings—international symposium on electrets, 5th, pp 565–570
16. Mellinger A, Singh R, Wegener M, Wirges W, Suarez RF, Lang SB et al (2005) High-resolution three-dimensional space-charge and polarization mapping with thermal pulses. In: Proceeding—international symposium on electrets (ISE 12), 12th, Salvador, Brazil, September 11–14, 2005, pp 212–215
17. Gol'tsov YI, Kramarenko IS, Panchenko EM, Zagoruiko VA, Mal'tsev VT, Sokolova TV (1983) Electret effect in heterogeneous ceramic dielectrics and glasses. USSR Avail VINITI Deposited Doc (VINITI 2386-83), 19 pp
18. Gubkin AN, Popova OS, Ogloblin VA, Kuskova AM (1974) Study of electrect from ceramic dielectrics, glasses and glass-ceramics. Sb Ref—Vses Konf Fiz Dielektr Perspekt Ee Razvit, Meeting Date 1973, vol 2, pp 126–127
19. Gubkin AN, Kashtanova AM, Ogloblin VA, Rastorgueva AV (1972) Time dependences of charges and slowly established polarization of electrets made of glasses and glass-ceramics. USSR Tr Mosk Inst Elektron Mashinostr 21:38–47
20. Nakamura S, Ueshima M, Kobayashi T, Yamashita K (2003) Crystal growth modification by surface charge on ceramic electret in simulated body fluid. In: Key engineering materials, pp 240–242. Bioceramics 445–448
21. Panchapakesan R (2007) Electret effect in cement. Thesis, University at Buffalo, State University of New York
22. Huang C-Y, Chung DDL (in press) Controlling and increasing the inherent voltage in cement paste. Adv Cement Res
23. Wen S, Chung DDL (2007) Piezoresistivity-based strain sensing in carbon fiber reinforced cement. ACI Mater J 104(2):171–179
24. Wen S, Chung DDL (2006) Self-sensing of flexural damage and strain in carbon fiber reinforced cement and effect of embedded steel reinforcing bars. Carbon 44(8):1496–1502. doi:10.1016/j.carbon.2005.12.009
25. Wen S, Chung DDL (2006) Model of piezoresistivity in carbon fiber cement. Cement Concr Res 36(10):1879–1885. doi:10.1016/j.cemconres.2006.03.029
26. Zhu S, Chung DDL (2007) Theory of piezoresistivity for strain sensing in carbon fiber reinforced cement under flexure. J Mater Sci 42(15):6222–6233. doi:10.1007/s10853-006-1131-3
27. Wen S, Chung DDL (2006) Effects of strain and damage on the strain sensing ability of carbon fiber cement. J Mater Civ Eng 18(3):355–360. doi:10.1061/(ASCE)0899-1561(2006)18:3(355)
28. Wen S, Chung DDL (2005) Strain sensing characteristics of carbon fiber reinforced cement. ACI Mater J 102(4):244–248
29. Chung DDL (2002) Piezoresistive cement-based materials for strain sensing. J Intell Mater Syst Struct 13(9):599–609
30. Wen S, Chung DDL (2003) A comparative study of steel- and carbon-fibre cement as piezoresistive strain sensors. Adv Cement Res 15(3):119–128. doi:10.1680/adcr.15.3.119.36621
31. Wen S, Chung DDL (2002) Piezoelectric cement-based materials with large coupling and voltage coefficients. Cement Concr Res 32(3):335–339. doi:10.1016/S0008-8846(01)00682-2
32. Sun M, Li Z, Song X (2004) Piezoelectric effect of hardened cement paste. Cement Concr Compos 26:717–720. doi:10.1016/S0958-9465(03)00104-5
33. Sun M, Liu Q, Li Z, Wang E (2002) Electrical emission in mortar under low compressive loading. Cement Concr Res 32:47–50. doi:10.1016/S0008-8846(01)00627-5

34. Lam KH, Chan HLW (2005) Piezoelectric cement-base 1-3 composites. Appl Phys A 81:1451–1454. doi:10.1007/s00339-005-3226-0
35. Zhang D, Li Z, Wu K-R (2002) 2-2 piezoelectric cement matrix composite: part II actuator effect. Cement Concr Res 32:825–830
36. Cheng X, Huang S, Chang J (2007) Piezoelectric, dielectric and ferroelectric properties of 0-3 ceramic/cement composites. J Appl Phys 101:094110. doi:10.1063/1.2730559
37. Cheng X, Huang S, Chang J, Lu L, Liu F (2005) Dielectric and piezoelectric properties of piezoelectric ceramic-sulphoaluminate cement composites. Smart Mater Struct 14(59-N):63
38. Dong B, Li Z (2005) Cement-based piezoelectric cement smart composites. Compos Sci Technol 65:1363–1371. doi:10.1016/j.compscitech.2004.12.006
39. Gerhard-Multhaupt R, Künstler W, Görne T, Pucher A, Weinhold T, Seiß M (2000) Porous PTFE space-charge electrets for piezoelectric applications. IEEE Trans Dielectr Electr Insul 7(4):480–488. doi:10.1109/94.868065
40. Mellinger A, Gonzalez FC, Gerhard-Multhaupt R, Santos LF, Faria RM (2002) Photostimulated discharge of corona and electron-beam charged electret polymers. In: Proceedings—international symposium on electrets, 11th, Melbourne, Australia, October 1–3, 2002, pp 7–10
41. Krashennikov AI, Lipaev SM, Rybnikov YS, Sbrodova LI (1986) Triboelectret effect during triboelectrification of power coatings. USSR, Lakokrasochnye Materialy i Ikh Primenenie 3:38–40
42. Bally RJ (1987) Cement–sodium silicate suspensions for underground construction. Hidrotehnica 32(7):260–265
43. Winter E, Clarke WJ, Guthrie JW (1986) Microfine cement grout strengthens foundations. Concr Int Des Constr 8(10):59–61
44. Domone PL (1990) The properties of low-strength silicate/Portland cement grouts. Cement Concr Res 20(1):25–35. doi:10.1016/0008-8846(90)90113-C
45. Lim HM, Yang HC, Chun BS, Lee SH (2005) The effect of sodium tripolyphosphate on sodium silicate-cement grout. In: Materials science forum, pp 486–487. Eco-Mater Process Des VI, 391–394
46. Scheetz BE, Hoffer JP (1995) Characterization of sodium silicate-activated Portland cement: 1. Matrixes for low-level radioactive waste forms. American Concrete Institute, SP-158 (Concrete and Grout in Nuclear and Hazardous Waste Disposal), pp 91–110
47. Okamoto T (1981) Acid-resistant cement prepared from sodium silicate binder. Semento Gijutsu Nenpo 35:90–93
48. Morioka M (2006) Cement admixtures for decreasing crack formation and cement composition. Jpn Kokai Tokkyo Koho, 9 pp
49. Larosa-Thompson J, Gill P, Scheetz BE, Silsbee MR (1997) Sodium silicate application for cement and concrete. In: Proceeding of the international congress on the chemistry of cement, 10th, Gothenburg, June 2–6, 1997, 3 3iii024, 8 pp
50. Askeland DR, Phule PP (2003) The science and engineering of materials, 4th edn. Thomson, CA